Kinetic Studies of Dimeric Ncd: Evidence That Ncd Is Not Processive†

Kelly A. Foster and Susan P. Gilbert*

Department of Biological Sciences, 518 Langley Hall, University of Pittsburgh, Pittsburgh, Pennsylvania 15260

Received June 29, 1999; Revised Manuscript Received November 27, 1999

ABSTRACT: Ncd is a kinesin-related motor protein which drives movement to the minus-end of microtubules. The kinetics of Ncd were investigated using the dimeric construct MC1 (Leu^{209}−Lys^{700}) expressed in *Escherichia coli* strain BL21(DE) as a nonfusion protein [Chandra, R., Salmon, E. D., Erickson, H. P., Lockhart, A., and Endow, S. A. (1993) *J. Biol. Chem. 268*, 9005−9013]. Acid chemical quench flow methods were used to measure directly the rate of ATP hydrolysis, and stopped-flow kinetic methods were used to determine the kinetics of mantATP binding, mantADP release, dissociation of MC1 from the microtubule, and binding of MC1 to the microtubule. The results define a minimal kinetic mechanism, $M{\cdot}N + ATP \overset{1}{\rightleftharpoons} M{\cdot}N{\cdot}ATP \overset{2}{\rightleftharpoons} M{\cdot}N{\cdot}ADP{\cdot}P \overset{3}{\rightleftharpoons} N{\cdot}ADP{\cdot}P \overset{4}{\rightleftharpoons} N{\cdot}ADP + P \overset{5}{\rightleftharpoons} M{\cdot}N{\cdot}ADP \overset{6}{\rightleftharpoons} M{\cdot}N + ADP$, where N, M, and P represent Ncd, microtubules, and inorganic phosphate respectively, with $k_{+1} = 2.3$ μM^{-1} s^{-1}, $k_{+2} = 23$ s^{-1}, $k_{+3} = 13$ s^{-1}, $k_{+5} = 0.7$ μM^{-1} s^{-1}, and $k_{+6} = 3.7$ s^{-1}. Phosphate release (k_{+4}) was not measured directly although it is assumed to be fast relative to ADP release because Ncd is purified with ADP tightly bound at the active site. ATP hydrolysis occurs at 23 s^{-1} prior to Ncd dissociation at 13 s^{-1}. The pathway for ATP-promoted detachment (steps 1−3) of Ncd from the microtubule is comparable to kinesin's. However, there are two major differences between the mechanisms of Ncd and kinesin. In contrast to kinesin, mantADP release for Ncd at 3.7 s^{-1} is the slowest step in the pathway and is believed to limit steady-state turnover. Additionally, the burst amplitude observed in the pre-steady-state acid quench experiments is stoichiometric, indicating that Ncd, in contrast to kinesin, is not processive for ATP hydrolysis.

Ncd[1] is a member of the kinesin superfamily of motor proteins which translocate along microtubules by coupling ATP hydrolysis to force production (*2*, *3*). Conventional kinesin, the founding member of the kinesin superfamily, moves membranous organelles from the neuron cell body to the synapse by driving movement to the plus-end of microtubules (*4*, *5*). Ncd, on the other hand, is responsible for spindle organization and integrity during female meiosis and during the early cleavages of the *Drosophila melanogaster* embryo. Therefore, Ncd is a molecular motor that moves one microtubule relative to another by generating minus-end directed movement (*6*, *7*). Ncd and kinesin also differ in their motility and ATPase rates: Ncd is a much slower motor with respect to both aspects than kinesin. Additionally it has been reported that Ncd is not as highly processive as kinesin (*8*−*10*). Howard et al. (*11*) reported in 1989 that a single kinesin molecule is sufficient to move a microtubule in motility assays, and the observation of a super-stoichiometric phosphate burst published in 1995 confirmed that kinesin is a chemically processive ATPase (*12*). Ncd, on the other hand, requires ∼4 motors/microtubule to produce movement (*10*), and motility assays indicate that Ncd does not move processively along the microtubule (*9*, *10*). However, to date, there is little evidence that the dimeric Ncd motor is not chemically processive. Additionally, the possibility that single Ncd molecules are moving microtubules below the limit of resolution of the motility assays cannot be excluded.

The numerous differences between Ncd and kinesin are surprising in light of the high structural homology of the motor domains (∼320 amino acids). The amino acid sequences are ∼40% identical, and the three-dimensional crystal structures of the single motor domains are nearly superimposable (*13*, *14*). However, comparison of the recently solved kinesin and Ncd dimer structures suggests that, despite the structural similarity of the catalytic domains, there is a different overall orientation of the heads of Ncd in comparison to kinesin (*15*, 16). The unique structures of Ncd and kinesin due to dimerization of the motor domains may contribute to the mechanistic differences observed between these molecular motors.

For kinesin, Gilbert, Moyer, and Johnson (*12*, *17*) reported that dissociation was the rate-limiting step in the ATPase

† This work was supported by Grant GM 54141 to S.P.G. from the National Institutes of Health, Grant IRG-58-35 from the American Cancer Society, and in part by a Basil O'Connor Starter Scholar Research Award (5-FY95-1136) from the March of Dimes Birth Defects Foundation. S.P.G. is also the recipient of an American Cancer Society Junior Faculty Research Award (JFRA-618). K.A.F. is a University of Pittsburgh Chancellor's Scholar and the recipient of a Beckman Scholarship from the Arnold and Mabel Beckman Foundation and a Barry M. Goldwater Scholarship in support of undergraduate research.

* To whom correspondence should be addressed. Phone: (412) 624-5842. Fax: (412) 624-4759. E-mail: spg1+@pitt.edu.

[1] Abbreviations: Ncd, nonclaret disjunctional; MC1, Ncd construct consisting of amino acid residues Leu^{209}-Lys^{700}; Hepes, *N*-[2-hydroxyethyl]piperzaine-*N*′-[2-ethanesulfonic acid]; MgAcetate, magnesium acetate; KAcetate, potassium acetate; Mt·N, Microtubule·Ncd complex; DTT, dithiothreitol; 3′-dATP, cordycepin 5′-triphosphate; 2′-dATP, 2′-deoxyadenosine 5′-triphosphate; mantADP, 2′(3′)-*O*-(*N*-methylanthraniloyl)adenosine 5′-diphosphate; mantATP, 2′(3′)-*O*-(*N*-methylanthraniloyl)adenosine 5′-triphosphate; P_i, inorganic phosphate.

10.1021/bi991500b CCC: $19.00
Published on Web 01/28/2000

cycle while ADP release occurred rapidly. Ma and Taylor (*18*, *19*), however, reported that ADP release was much slower and did make a contribution to limiting the steady-state rate of the ATPase cycle. For a monomeric Ncd construct, Pechatnikova and Taylor (*20*) reported that ADP release occurred extremely slowly and was rate limiting, and their recent report on the Ncd dimer also revealed ADP release to be the slowest step in the pathway (*21*). The evidence suggests that the rate-limiting step in the ATPase cycle of kinesin and Ncd may differ.

This work was undertaken to provide a detailed kinetic analysis of the ATPase mechanism of a dimeric Ncd construct. The results presented here establish a minimal kinetic scheme for the Mt·Ncd ATPase. There are two major differences between the ATPase cycles of kinesin and Ncd. First, Ncd is not a processive ATPase while kinesin is processive. Additionally, ADP release is the rate-limiting step in the Ncd ATPase cycle with motor dissociation from the microtubule occurring relatively quickly. The kinetics for MC1 also suggest that the motor domains are not strictly independent of each other.

EXPERIMENTAL PROCEDURES

Materials. [α-^{32}P]ATP (>3000 Ci/mmol) was purchased from NEN Life Science Products, PEI-cellulose F TLC plates (EM Science of Merck, 20 × 20 cm, plastic backed) from VWR Scientific (West Chester, PA), and Taxol (*Taxus brevifolia*) from Calbiochem. ATP, GTP, DEAE-Sepharose FF, and SP-Sepharose were obtained from Pharmacia Biotech, Inc. (Uppsala, Sweden).

Buffer Conditions. The following buffer was used for the experiments described: ATPase buffer at 25 °C (20 mM Hepes, pH 7.2, with KOH, 0.1 mM EDTA, 0.1 mM EGTA, 5 mM MgAcetate, 50 mM KAcetate, 1 mM DTT, and 5% sucrose).

Protein Purification. The dimeric Ncd construct (MC1) was expressed in the *E. coli* cell line BL21(DE3) from a clone (*1*) generously provided by Sharyn Endow, Duke University Medical Center. This MC1 construct is expressed as a nonfusion protein and contains amino acid residues Leu^{209}−Lys^{700}; therefore, the N-terminal ATP-independent microtubule binding site is absent. MC1 was purified and characterized as described previously (*22*). The protein concentration of purified MC1 was determined by the Bradford method (Bio-Rad Protein Assay, IgG as standard) and spectrophometrically at A_{280} and at A_{259} to determine the concentration of the stoichiometrically bound ADP (*22*). Four different MC1 preparations were used for the pre-steady-state experiments reported. Each preparation was characterized for active-site concentration (*22*) and steady-state turnover. The steady-state parameters were comparable for the four preparations: $k_{cat} = 1.96 \pm 0.06$ s^{-1}, $K_{m,ATP} = 23.1 \pm 1.8$ μM, and $K_{1/2,Mt} = 20.5 \pm 1.75$ μM. The K_d for dimerization for MC1 (<5 nM) was determined by equilibrium sedimentation centrifugation and reported previously (*22*). The MC1 concentration used in the pre-steady-state experiments was significantly greater than 5 nM; therefore, MC1 is dimeric under the conditions of these experiments. For the steady-state and pre-steady-state experiments reported, we have not pretreated the Mt·N complex to remove bound ADP or ADP released from the active site into solution. This approach was chosen due to concern that Ncd protein behavior may be altered by the treatment and concern that a significant concentration of inactive MC1 would be present in the reactions because of the loss of activity associated with removal of nucleotide from the active site. For MC1, the acid quench experiments showing full burst amplitude (Figure 2) indicate that incubation with microtubules to form the Mt·N complex does activate ADP release from the active sites of MC1.

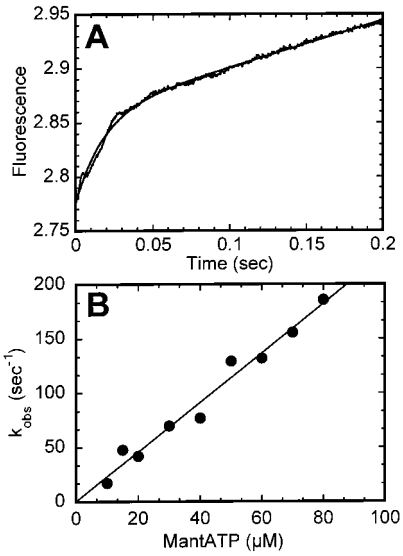

FIGURE 1: MantATP binding to the Mt·N complex. The preformed Mt·N complex (20 μM tubulin, 6 μM MC1) was rapidly mixed in the stopped-flow instrument with varying concentrations of mantATP (10−80 μM). All concentrations refer to final concentration of reactants after mixing. (A) A representative stopped-flow transient, the average of four individual traces, was obtained after mixing the Mt·N complex with 40 μM mantATP. The smooth line shows the fit of the data to a single-exponential plus a linear term which provides $k_{obs} = 76.0 \pm 1.3$ s^{-1} for the initial exponential phase and 0.4 s^{-1} for the slow phase. (B) The rate constant of the initial exponential phase for each transient was plotted as a function of mantATP concentration. The data were fit to a straight line yielding the second-order rate constant, $k_{+1} = 2.3 \pm 0.1$ μM^{-1} s^{-1}. The rate of slow phase of fluorescence enhancement is essentially independent of mantATP concentration and varied from 0.25 to 0.45 s^{-1}.

On the day of each experiment, the microtubules were assembled from soluble tubulin (cold depolymerized and clarified by centrifugation) and stabilized with 20 μM Taxol as described previously (*23*). This procedure yielded microtubules that were competent for polymerization with essentially no soluble tubulin remaining.

Fluorescence Nucleotide Analogues. The *N*-methylanthraniloyl derivatives of adenine nucleotides were synthesized (*24*) and characterized as described previously (*17*, *25*). In the experiments reported here, we used different mant isomers: 2′mant-3′dATP, 3′mant-2′dATP, the mixture of 2′- and 3′-isomers of mantATP (mantATP), and the mixture of 2′- and 3′-isomers of mantADP (mantADP). The two isomers in mantATP (or mantADP) differ from the pure isomers in that a hydroxyl group is attached to the 2′- or 3′-carbon of the ribose.

Acid Quench Experiments. The rate constant of ATP hydrolysis was measured using a rapid chemical quench-flow instrument (KinTek Corp., Austin, TX) at 25 °C in ATPase buffer. ATP hydrolysis was measured by rapidly mixing the preformed Mt·N complex (20 μM tubulin, 5 μM

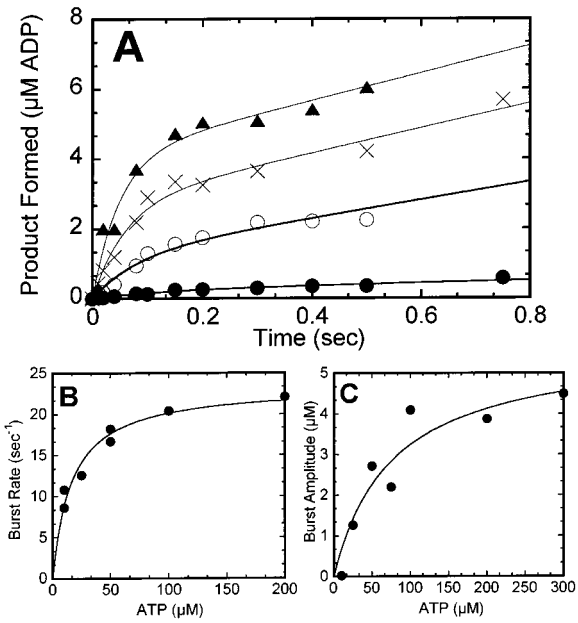

FIGURE 2: Pre-steady-state ATP hydrolysis by MC1. The preformed Mt·N complex (5 μM MC1, 20 μM tubulin) was rapidly mixed in the chemical quench flow instrument with varying concentrations of [α-^{32}P]MgATP and allowed to react for 0.01−2 s as described in the Experimental Procedures. All concentrations reported are final after mixing. (A) The transients for ATP hydrolysis in the presence of 10 μM (●), 25 μM (○), 50 μM (×), and 100 μM (▲) [α-^{32}P]-MgATP. The data were fit to the burst equation (eq 1). Only the initial 0.8 s of each transient is shown to expand the time domain of the initial burst phase. (B) The pre-steady-state kinetic burst rate constant calculated for each transient and plotted as a function of [α-^{32}P]MgATP concentration. The data were fit to a hyperbola which yields $k_{+2} = 23.4 \pm 1.2$ s^{-1} and $K_{d,ATP} = 16.4 \pm 3.1$ μM. The [α-^{32}P]MgATP concentrations used were sufficiently high such that ATP binding (k_{+1}) no longer limits the rate of the first turnover. Therefore, the maximum rate constant for the burst predicts the maximum rate constant for ATP hydrolysis (k_{+2}). (C) The amplitude of the pre-steady-state burst plotted as a function of [α-^{32}P]MgATP concentration. The data were fit to a hyperbola (maximum burst amplitude = 5.7 ± 1.1 μM). Panels B and C contain data from experiments not shown in panel A.

MC1, and 20 μM Taxol, final after mixing) with increasing concentrations of [α-^{32}P]ATP. The reaction was quenched with 2 N HCl and expelled from the instrument. Chloroform (100 μL) was immediately added and vortexed to denature the protein. The reaction was then neutralized with 2 M Tris/3 N NaOH to pH 7.2−8.0. An aliquot (1.5 μL) of each reaction mixture was spotted onto a PEI-cellulose TLC plate and subsequently developed with 0.6 M potassium phosphate buffer, pH 3.4, with phosphoric acid. Radiolabeled nucleotide was quantified using a FUJI Bas-2000 PhosphorImager (Fuji Photo Film Co., Ltd). The acid quench liberated bound nucleotide and products from the active site of MC1. Thus, the product formed at each time point represents the sum of N·[α-^{32}P]ADP·P$_i$, N·[α-^{32}P]ADP, and [α-^{32}P]ADP released from the active site of the enzyme and free in solution. The data were analyzed by nonlinear regression using KaleidaGraph software (Synergy Software, Reading, PA).

The time course of ATP hydrolysis was fit to the biphasic burst equation

$$\text{product} = A[1 - \exp(-k_b t)] + k_2 t \quad (1)$$

where A is the amplitude of the burst representing the formation of [α-^{32}P]ADP·P$_i$ at the active site, k_b is the rate constant of the pre-steady-state burst phase, k_2 is the rate constant of the linear phase and corresponds to steady-state turnover, and t is the time in seconds.

Stopped-Flow Kinetics. The kinetics of mantATP binding, mantADP release, dissociation of MC1 from the microtubule, and binding of MC1 to the microtubule were measured using a KinTek Stopped-Flow Instrument (model SF-2001, KinTek Corp., Austin, TX) equipped with a 100 W Hg arc lamp at 25 °C in ATPase buffer. Each trace shown is an average of four to eight traces. For experiments with the nucleotide analogues mantATP and mantADP, the fluorescence emission at 450 nm was monitored using a 400 nm cutoff longwave pass filter with excitation at 360 nm. The dissociation kinetics of the Mt·MC1 complex and the binding kinetics of MC1 to microtubules were determined by turbidity measurements at 340 nm. The kinetic transients were fit to a single-exponential function plus a linear term using KinTek software (version 5.28).

The mantATP binding data in Figure 1B were fit to a straight line such that

$$k_{obs} = k_{+1}[\text{mantATP}] + k_{-1} \quad (2)$$

where k_{obs} is the rate constant obtained from the exponential phase of the fluorescence change, k_{+1} defines the second-order rate constant for mantATP binding, and k_{-1}, obtained from the y-intercept, corresponds to the rate of mantATP release. The dissociation equilibrium constant is defined by

$$K_d = k_{-1}/k_{+1} \quad (3)$$

RESULTS

MantATP Binding to Mt·MC1 Complex. We began our analysis of the ATPase mechanism of Ncd by measuring the pre-steady-state kinetics of mantATP binding to the Mt·MC1 complex. MantATP and mantADP are considered to be good fluorescence analogues for Ncd because the ATPase and mantATPase activities are very similar (*26*). The steady-state k_{cat} and $K_{1/2,Mt}$ for Ncd are nearly the same in the presence of either ATP or mantATP. The preformed Mt·N complex (20 μM tubulin and 6 μM MC1, final after mixing) was rapidly mixed with varying concentrations of mantATP (10−80 μM) in the stopped-flow, and the change in fluorescence was monitored. The enhancement in fluorescence is associated with mantATP leaving the hydrophilic buffer environment and entering the more hydrophobic active site of the enzyme. Figure 1A shows that mantATP binding (mixture of 2′- and 3′-mantATP isomers) provides a biphasic fluorescence change: a fast exponential increase in fluorescence followed by a slower increase in fluorescence at 0.43 s^{-1}. As the mantATP concentration was increased, the rate constant of the exponential phase increased linearly as shown in Figure 1B. The observed rate at 80 μM mantATP was 186 s^{-1}. Deterioration of the signal relative to noise precluded measurements at higher mantATP concentrations. The slope provides the second-order rate constant for mantATP binding, k_{+1} at 2.3 μM^{-1} s^{-1}, and no significant y-intercept is present. Because $k_{obs} = k_1$[mantATP] + k_{-1} (eq 2), the data indicate that there is not an appreciable k_{-1}. These data suggest that mantATP binds to the Mt·MC1 complex (Scheme 1) such that there is not significant partitioning of the Mt·N·ATP

Scheme 1: Mt·N ATPase Mechanism

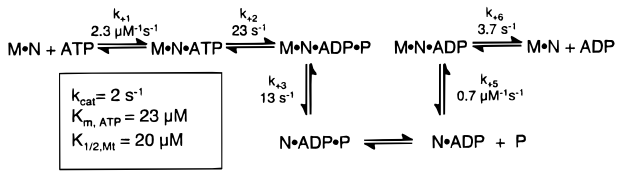

Table 1: MantATP Binding Kinetic Constants[a]

substrate	k_{+1}	k_{-1} (s^{-1})	K_d (μM)
2′mant-3′dATP	$1.0 \pm 0.03\ \mu M^{-1}\ s^{-1}$	6.1 ± 1.5	6.1
3′mant-2′dATP	$2.7 \pm 0.3\ \mu M^{-1}\ s^{-1}$	22.8 ± 8.7	8.5
mantATP	$2.3 \pm 0.12\ mM^{-1}\ s^{-1}$		

[a] Kinetic constants of mantATP binding to the Mt·N complex where k_{+1} is the second-order rate constant for mantATP binding, k_{-1} is the off rate for mantATP, and K_d is the dissociation constant for mantATP. Conditions were as follows: 20 mM Hepes, pH 7.2 with KOH, 5 mM MgAcetate, 0.1 mM EDTA, 0.1 mM EGTA, 50 mM KAcetate, 1 mM DTT, 5% sucrose at 25 °C.

intermediate between the forward and reverse steps as observed for kinesin (*27*). A mantATP concentration dependence was not evident for the second phase of the fluorescence transient (Figure 1A), and the rate constants were too slow (0.25−0.45 s^{-1}) to be attributed to ATP hydrolysis.

The mantATP-binding experiments were also performed with 2′mant-3′dATP and 3′mant-2′dATP (Table 1). The results show that the kinetics of mantATP binding were similar for the 2′mant-3′dATP derivative and the mantATP mixture. However, the 3′mant-2′dATP isomer exhibited a slightly higher second-order rate constant for binding at 2.7 $\mu M^{-1}\ s^{-1}$ and a significant k_{-1} at 23 s^{-1}. Additionally, the binding kinetics with the 3′mant-2′dATP isomer were biphasic with an exponential increase in fluorescence followed by a slight decrease in fluorescence (data not shown) as observed previously for dimeric kinesin and monomeric Ncd (*18*, *20*, *28*). The 3′mant-2′dATP isomer, because of the higher k_{-1}, was not used in subsequent stopped-flow experiments. The rate and equilibrium constants for the three mantATP analogues are summarized in Table 1.

Time Course of ATP Hydrolysis. Acid quench experiments were performed as a function of [α-^{32}P]MgATP concentration to determine the rate constant of ATP hydrolysis. The preformed Mt·N complex (5 μM MC1, 20 μM tubulin) was rapidly mixed with [α-^{32}P]ATP. Figure 2A shows the time course of ATP hydrolysis by MC1 at four different ATP concentrations. The initial burst of product formation during the first ATP turnover represents the formation of the N·ADP·P_i intermediate. This exponential burst phase is then followed by a slower rate of ADP production corresponding to steady-state turnover. The presence of a pre-steady-state burst indicates that the rate-limiting step in the ATPase mechanism occurs after ATP hydrolysis. The data were fit to the burst equation (eq 1) which revealed an increase in the burst rate and amplitude with increasing ATP concentration. The rate constants of the linear phase obtained from this fit are consistent with the predicted steady-state rate constants at the enzyme, microtubule, and ATP concentrations used in the experiment.

In Figure 2B, the burst rate obtained from the exponential phase is plotted as a function of ATP concentration. At high ATP concentrations, ATP binding no longer limits the rate of the first turnover. Therefore, the maximum rate constant of the burst phase obtained from the fit of the data to a hyperbola provides the rate constant for ATP hydrolysis, $k_{+2} = 23\ s^{-1}$ and the $K_{d,ATP}$ at 16.4 μM (Scheme 1). Although the microtubule concentration used in the acid quench experiments is high at 20 μM tubulin, this concentration is not saturating for steady-state turnover. Experiments at varying microtubule concentrations show that k_{+2} does not change appreciably as a function of microtubule concentration in the range 12−30 μM tubulin (data not shown). These results indicate that, for the first turnover of ATP, what is required for full activation of ATP hydrolysis is a microtubule concentration that is sufficiently high to ensure MC1 is bound to the microtubule. Experiments at microtubule concentrations of ≥35 μM tubulin were attempted but were inaccurate due to the inability to achieve thorough mixing of the viscous Mt·MC1 solution within a few milliseconds.

Figure 2C shows the burst amplitudes obtained from eq 1 and plotted as a function of ATP concentration. Note that the maximum burst amplitude determined at 300 μM ATP is 4.5 μM, suggesting approach to a full burst amplitude of 5 μM. The fact that the burst amplitude saturates at the enzyme concentration is indicative of relatively tight ATP binding which is consistent with the low k_{-1} observed in the mantATP-binding experiment.

In addition to the acid quench experiments at 5 μM MC1 + 20 μM tubulin, experiments were also performed at 5 μM MC1 + 12 μM tubulin, 10 μM MC1 + 30 μM tubulin, and 1 μM MC1 + 20 μM tubulin with ATP concentrations varying from 25 to 600 μM. There was no evidence of a super-stoichiometric burst of ADP·P_i formation at any of these experimental conditions. These data indicate that Ncd is not a processive ATPase, consistent with the motility results which document dimeric Ncd's lack of processive movement (*9*, *10*).

ATP-Promoted Dissociation of MC1 from the Microtubule. We next measured the rate of MC1 dissociation from the microtubule using the stopped-flow instrument to monitor changes in turbidity (Figure 3). The preformed Mt·N complex (2.5 μM MC1, 2.3 μM tubulin) was rapidly mixed with varying concentrations of MgATP (7.5−750 μM). Figure 3B shows the rate constants obtained from each initial exponential phase plotted as a function of MgATP concentration. Fitting the data to a hyperbola provides the k_{+3} at 13 s^{-1} with the $K_{1/2,ATP}$ at 19 μM. Our interpretation of the pathway for dissociation is that ATP binding and ATP hydrolysis occur first, followed by detachment of the motor from the microtubule. This interpretation is based on several lines of evidence. First, the dissociation step at 13 s^{-1} is slower than ATP hydrolysis at 23 s^{-1}, but the difference in these rate constants is not large enough to order these steps to define the pathway. However, Foster et al. (*22*) reported that the only nucleotide intermediate weakly bound to microtubules was the N·ADP·P_i intermediate and that the nonhydrolyzable analogue AMP-PNP did not promote Ncd dissociation from the microtubule. These data are all consistent with the interpretation that ATP hydrolysis occurs first, followed by detachment of the N·ADP·P_i intermediate from the microtubule (Scheme 1). Furthermore, Figure 3A shows a small lag in the kinetics prior to the decrease in turbidity which we attribute to the time required for ATP binding and hydrolysis prior to dissociation. The $K_{1/2,ATP}$ for

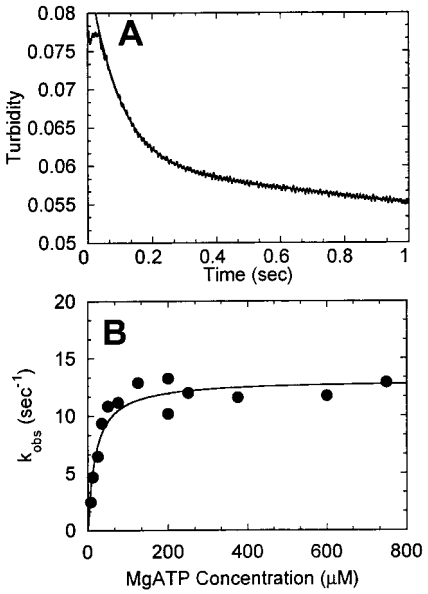

FIGURE 3: ATP promoted dissociation of the Mt·N complex. The preformed Mt·N complex (2.3 μM tubulin, 2.5 μM MC1) was rapidly mixed with varying concentrations of MgATP (7.5−750 μM) in the stopped-flow instrument. (A) A representative stopped-flow record consisting of six averaged traces showing the time course after mixing the Mt·N complex with 375 μM MgATP. The smooth line shows the fit of the data to a single-exponential plus a linear term. The fast exponential phase provides $k_{obs} = 11.6 \pm 0.1$ s^{-1}. (B) The rate constant of the exponential phase for each transient was plotted as a function of MgATP concentration. The data were fit to a hyperbola which provides the maximum rate constant $k_{obs} = 13.1 \pm 0.6$ s^{-1} and $K_{1/2,ATP} = 18.7 \pm 4.1$ μM.

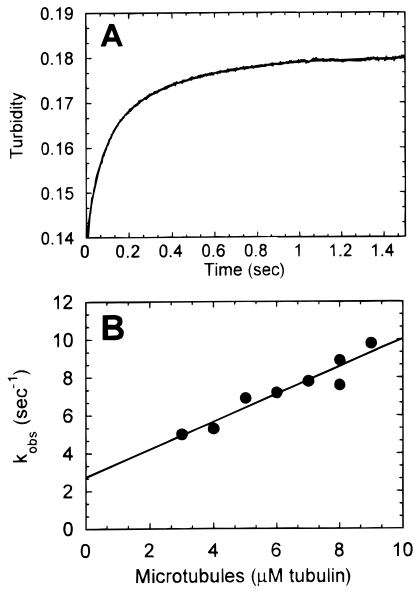

FIGURE 4: Binding of MC1 to microtubules. MC1 (4 μM) was rapidly mixed with varying concentrations of microtubules (3−9 μM) in the stopped-flow instrument. All concentrations are final after mixing. (A) A representative stopped-flow record at 8 μM microtubules consisting of six averaged traces. The smooth line shows the fit of the data to a single-exponential plus a linear term: $k_{obs} = 9.0 \pm 0.1$ s^{-1} of the initial exponential phase. (B) The rate constant obtained from the initial fast phase of each transient plotted as a function of microtubule concentration. The data were fit to a straight line, and the slope provides the $k_{+5} = 0.7 \pm 0.1$ μM^{-1} s^{-1} and the *y*-intercept, the $k_{-5} = 2.7 \pm 0.6$ s^{-1}.

the dissociation step at 19 μM corresponds to the $K_{d,ATP}$ for the hydrolysis step at 16 μM, suggesting that no partitioning of the Mt·N·ATP intermediate occurs. These results indicate that the steps of ATP binding, ATP hydrolysis, and dissociation of N·ADP·P$_i$ from the microtubule occur directly without significant reversals at step 2 (ATP hydrolysis) or step 3 (Ncd dissociation).

We also performed the dissociation kinetic experiments with an additional 100 mM KCl added to the ATP syringe. In the case of kinesin, the added salt was required to weaken rebinding of the motor to the microtubule after detachment in order that the dissociation kinetics could be measured (*12*). For MC1, there was no difference in rate of the exponential phase or the amplitude of the exponential phase measured in the presence (150 mM final) or absence (50 mM final) of the added salt. These results are consistent with the interpretation that ATP promotes complete detachment of the Ncd dimer from the microtubule and Ncd is not a highly processive motor.

Binding of MC1 to Microtubules. Because monomeric and dimeric Ncd motors are purified with ADP bound at the active site, it has been assumed that the N·ADP intermediate rebinds the microtubule. We measured the rate of formation of the Mt·N complex using the stopped-flow instrument to monitor changes in turbidity (Figure 4). MC1 at 4 μM was rapidly mixed with varying concentrations of microtubules (3−9 μM). The rate of binding increased linearly with microtubule concentration as shown in Figure 4B. Fitting the data to a straight line yields the second-order rate constant for microtubule association, k_{+4}, at 0.7 μM^{-1} s^{-1}, and the *y*-intercept provides an off rate, k_{-4}, at 2.7 s^{-1}. The dissociation constant is defined by $K_d = k_{off}/k_{on}$. On the basis of the microtubule-binding results reported in Figure 4, the apparent K_d is 3.9 μM. This equilibrium constant is significantly lower than the $K_{1/2,Mt}$ obtained from steady-state experiments where $K_{1/2,Mt} = 20$ μM, yet is significantly higher than the $K_{d,Mt}$ at 0.22 μM determined by equilibrium measurements in the absence of added ATP, ADP, or AMP-PNP (*22*). In addition, the microtubule association constant at 0.7 μM^{-1} s^{-1} is significantly higher than the apparent second-order rate constant at 0.1 μM^{-1} s^{-1} for microtubule activation of steady-state turnover obtained from the initial slope of the microtubule concentration dependence of the ATPase rate ($k_{cat}/K_{1/2,MT} = 2$ s^{-1}/20 μM). This apparent discrepancy suggests that these experiments are measuring different behaviors of the motor dependent upon the conditions. In the case of steady-state turnover of a nonprocessive motor, microtubule binding would be expected to be weaker because the motor releases after each cycle of ATP turnover and must rebind the microtubule. In the case of the stopped-flow turbidity measurement, we are measuring directly the single step in the absence of added ATP, ADP, or AMP-PNP. In the equilibrium-binding experiments, the reaction is allowed to come to equilibrium; therefore, initial rapid steps of binding and release are not observed—only the final state at equilibrium.

MantADP Release from MC1. To complete our analysis of the ATPase mechanism for Ncd, we measured the rate of mantADP release from MC1 as a function of microtubule concentration using the stopped-flow instrument (Figure 5). MC1 was incubated with mantADP in a 1:2 ratio in order to replace the ADP bound at both heads of MC1 with mantADP. The N·mantADP complex (2 μM MC1 and 4 μM

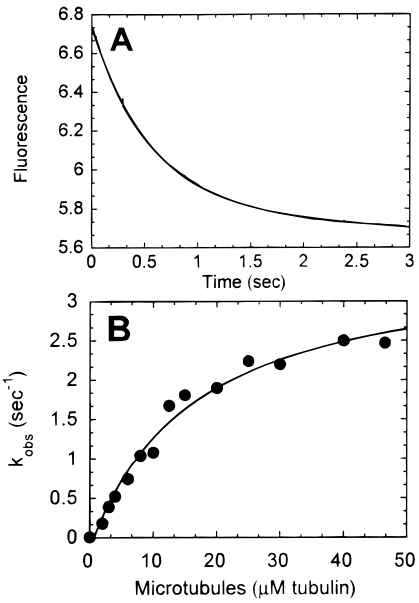

FIGURE 5: MantADP release from the Mt·N·MantADP complex. The MC1·mantADP complex (2 μM MC1, 4 μM mantADP) was preformed such that MC1 contained mantADP bound to both heads. This complex was rapidly mixed in the stopped-flow instrument with varying concentrations of microtubules (2−46.5 μM tubulin) plus 0.5 mM MgATP. (A) A representative stopped-flow record (5 averaged traces) at 15 μM microtubules. The smooth line shows the fit of the data to an exponential function plus a linear term. The rate constant of the initial exponential phase, $k_{obs} = 1.80 \pm 0.01$ s^{-1}. (B) The rate constant obtained from the exponential phase plotted as a function of microtubule concentration. In the absence of microtubules, the rate constant for mantADP release is 0.004 ± 0.000 01. Fit of the data to a hyperbola yields a $k_{+6} = 3.7 \pm 0.2$ s^{-1} with half-maximal stimulation occurring at 16.3 ± 3.4 μM microtubules.

mantADP) was rapidly mixed with varying concentrations of microtubules (2−46.5 μM) plus 0.5 mM MgATP. The MgATP blocks rebinding of mantADP to the active site once it is released. Figure 5A shows the time dependence of the fluorescence change, fit to a single-exponential function and linear term. Figure 5B shows that the exponential rate constant associated with the fluorescence change increased with increasing microtubule concentrations. Fitting the data to a hyperbola yields a maximum rate constant for mantADP release at 3.7 s^{-1}. The concentration of microtubules that provided half the maximal rate is 16.3 μM tubulin, and this constant is very similar to the steady-state $K_{1/2,Mt}$ at 20 μM. These results suggest that both assays are measuring the same rate-limiting step.

Our experiments have shown that the steady-state k_{cat} of ATP turnover is 2 s^{-1} for dimeric MC1 (*22*). The rate of mantADP release observed here at 3.7 s^{-1} is the slowest step we have observed in the ATPase cycle and is sufficiently slow to limit steady-state turnover for the Ncd ATPase cycle (Scheme 1). However, the results presented do not show that mantADP release is equivalent to ADP release although all data to date suggest that mant nucleotides are good representatives for ATP and ADP. The hypothesis that ADP release is rate limiting is also consistent with the pre-steady-state burst which was observed in the ATP hydrolysis experiments. This burst of product formation indicates that some step after ATP hydrolysis is rate limiting. While we have not determined the rate of inorganic phosphate release, we believe that it is unlikely that this step is slower than ADP release. Ncd is purified with ADP bound to the active site, and gel filtration experiments have been unsuccessful in detecting P_i at the active site (26). These results imply that P_i is released more quickly than ADP. Furthermore, equilibrium binding experiments (22) revealed that the MC1·ADP complex has a very low affinity for P_i, further suggesting that P_i release is faster than ADP release. Thus, all of the information to date is consistent with a model in which ADP release is the rate-limiting step in the ATPase mechanism.

DISCUSSION

The results reported here and previously (*22*) establish a minimal kinetic mechanism for the Mt·Ncd ATPase (Scheme 1). To begin the cycle, ATP binds to the Mt·N complex in a rapid step that leads to ATP hydrolysis at 23 s^{-1}. ATP hydrolysis is followed by detachment of Ncd from the microtubule which also occurs relatively quickly at 13 s^{-1}. This sequence of steps is also supported by equilibrium binding data which show that MC1 is detached from the microtubule only in the presence of ADP·P_i (*22*). Phosphate release is assumed to occur more rapidly than ADP release because Ncd is purified with ADP bound and because the equilibrium-binding experiments indicated a very weak K_d for inorganic phosphate. Rebinding at 0.7 μM^{-1} s^{-1} is then followed by slow ADP release at 3.7 s^{-1}.

Rate-Limiting Step. The burst in the pre-steady-state chemical quench data (Figure 2) indicates that some step after ATP hydrolysis is rate limiting. The rate of ADP release (Figure 5) is the slowest step that we measured, leading us to conclude that it is the rate-limiting step in the Ncd ATPase cycle. This conclusion is consistent with reports which examined the steady-state kinetic parameters of other Ncd constructs. Moore et al. (*29*) and Lockhart et al. (*30*) reported a slow rate of ADP release for the dimeric MC5 GST-fusion protein while Shimizu et al. (*26*) as well as Pechatnikova and Taylor (*20*) reported rate-limiting ADP release at 3.3 s^{-1} for a monomeric Ncd construct. More recently, Pechatnikova and Taylor (*21*) reported ADP release as the main rate-limiting step for their MC1 construct which is expressed as a GST-fusion protein. Because of the difference in the rate constant of ADP release which we measured at 3.7 s^{-1} and the steady-state k_{cat} for MC1 at 2 s^{-1}, we pursued additional experiments to evaluate possible hypotheses. Two explanations would account for the fact that the slowest step in the pathway is faster than steady-state turnover. First, it is possible that the number of active sites was overestimated in these experiments, leading us to underestimate the steady-state k_{cat}. Because the A_{259} which measures ADP bound at the active site and the Bio-Rad Assay which measures protein concentration are in close agreement, we believe that the protein concentration is a true reflection of the active-site concentration within experimental error. It is also possible that cooperative interactions between the heads, which have been shown to exist for Ncd (*22*), could account for the discrepancy between the steady-state k_{cat} and the rate constant for ADP release (k_{+6}). According to this hypothesis, the observed rate of ADP release in the stopped-flow experiments (Figure 5) is a combination of two different rates, one slower than 3.7 s^{-1} and one faster than 3.7 s^{-1} with the two rates corresponding to mantADP release from each motor domain of the dimer. Experiments which

measured mantADP release from each motor domain independently revealed that ADP release from one motor domain occurred rapidly with mantADP release from the partner motor domain at 1.4 s^{-1} (to be presented elsewhere), suggesting that steady state turnover was limited by ADP release. Similar experiments were performed and recently reported by Pechatnikova and Taylor (*21*). They also concluded that ADP release limits steady-state turnover.

Nonprocessive ATP Hydrolysis. The burst rate in the ATP hydrolysis experiments approaches 23 s^{-1} (Figure 2). The burst amplitude was greater than 4 μM at 100 μM ATP and saturated at ~5 μM which is equal to the enzyme concentration. A processive motor would be expected to hydrolyze multiple ATP molecules before reaching a steady-state level of dissociation, resulting in a super-stoichiometric burst. Ncd, however, does not display a super-stoichiometric burst at any of the ATP, microtubule, or MC1 concentrations that we examined, supporting the conclusion that Ncd is not a processive ATPase. This interpretation is consistent with data obtained from motility assays which do not show processive movement of Ncd molecules (*9*, *10*). Furthermore, DeCastro et al. (*10*) reported that ~4 Ncd dimeric motors are necessary for microtubule movement. Motility assays, however, cannot rule out the possibility of very low processive movement because they can only detect movement of 5−6 steps or more (>40 nm). The data presented here, however, suggest that Ncd is not even slightly processive. An alternative interpretation of these experiments is that Ncd is in fact processive, but we do not see a super-stoichiometric burst due to a fast ATP off rate. However, the mantATP binding experiments reveal that the k_{-1} is negligible, suggesting that the stoichiometric burst is truly reflecting a lack of processivity. As stated above, there are data to indicate that cooperative interactions between the motor domains of Ncd occur although we now know that this cooperativity does not lead to processive ATP turnover or processive movement.

Comparison to Kinesin. While Ncd bears a high structural similarity to kinesin in the core motor domain, recent crystal structures for dimeric kinesin and dimeric Ncd reveal a dramatic difference in the overall symmetry of the dimeric motors (*15*, *16*). In addition, the direction of movement, the motility behavior, and the cellular function of each motor differs, suggesting that there must be mechanistic differences between these microtubule-based motors. Therefore, it is worthwhile to examine the mechanistic differences and similarities between kinesin and Ncd. They both bind ATP relatively rapidly (*18*, *27*, *28*). However, dimeric Ncd appears to bind ATP more tightly with no evidence of a significant k_{-1} based on the mantATP binding data or the acid quench results for ATP hydrolysis (Figures 1 and 2B). In contrast, dimeric kinesin binds ATP much more weakly with $k_{-1} =$ 120 s^{-1} (*27*, *28*). Yet, both enzymes hydrolyze ATP rapidly relative to their steady-state turnover, and ATP hydrolysis occurs while the motor is bound to the microtubule. After ATP hydrolysis, crossbridge detachment from the microtubule occurs for both Ncd and kinesin (*12*, *18*, *27*).

For dimeric Ncd, dissociation occurs at 13 s^{-1} which is fast relative to the other steps in the cycle (Scheme 1). However, the experimental results for kinesin are more difficult to interpret. To measure the dissociation kinetics for either Ncd or kinesin, a Mt·motor complex was preformed and then rapidly mixed with ATP in the stopped-flow (*12*, *18*). The observed decrease in either light scattering or turbidity was measured, and the rate constant was determined for the exponential decrease as a function of ATP concentration. The same experiment by both Gilbert and Johnson (*12*) and Ma and Taylor (*18*) yielded a maximum rate constant of this ATP-dependent process at 12−14 s^{-1}. This step is rate-limiting for kinesin steady-state turnover because all other steps measured are fast relative to 12−14 s^{-1}. Furthermore, both groups have identified this point in the cycle as responsible for the force generating conformational changes required for movement. However, Taylor attributes this rate constant to conformational changes leading to P_i and ADP product release (*18*, *19*) whereas Gilbert, Moyer, and Johnson propose rate-limiting detachment of the kinesin head from the microtubule followed by rapid P_i release (*17*, *28*). Both hypotheses account for the data, and to date no direct experiments distinguishing the two hypotheses have been published.

Rebinding for both kinesin and Ncd occurs as the motor·ADP intermediate, but the second-order rate constant for kinesin is significantly higher (>10-fold) than rebinding for Ncd, suggesting that Ncd spends more of its ATPase cycle detached from the microtubule than kinesin. It has been proposed that one reason for kinesin's high processivity is the fact that it spends very little of its cycle detached from the microtubule (*11*, *31*). Thus, the kinetic results reported for dimeric Ncd support the mechanistic interpretation that Ncd spends a considerable amount of its duty cycle detached from the microtubule and is therefore not a processive molecular motor.

The rate-limiting step in the case of dimeric Ncd is ADP release. For kinesin, Ma and Taylor (*18*, *19*) reported ADP release for the first head at 50 s^{-1} with ADP release from the second motor domain at 100 s^{-1} in the presence of ATP. In contrast, Gilbert, Moyer, and Johnson (*17*, *28*) reported a fast rate of ADP release for both motor domains in the presence of ATP at ≥200 s^{-1}. The data reported here for Ncd as well as the results reported for kinesin suggest that there are distinct differences in the rate-limiting step for each motor that lead to mechanistic differences in force generation and possibly the reversed directionality of these motors. Studies to elucidate mechanistic contributions to directional bias for Ncd will be reported elsewhere.

Comparison to Myosin II and Dynein. In several aspects of its cycle, Ncd more closely resembles axonemal dynein and skeletal muscle myosin than it does to kinesin despite its high structural similarity to kinesin. The lack of processivity observed for Ncd is similar to that seen for myosin II, which also requires several motors to produce effective movement (*32*−*34*). Additionally, axonemal dynein and skeletal muscle myosin both show rate-limiting conformational changes linked to product release similar to Ncd (*25*, *35*−*40*). Ncd does, however, share some characteristics with kinesin that differ from those of dynein and myosin II. For both kinesin and Ncd, ATP binding and ATP hydrolysis occur on the microtubule prior to detachment. Additionally, skeletal muscle myosin (*35*) and axonemal dynein (*41*) both show extremely rapid release from their filament upon ATP binding (>1000 s^{-1}) while both Ncd and kinesin show slower dissociation (12−14 s^{-1}). Thus, Ncd appears to incorporate mechanistic aspects of myosin II, axonemal dynein, as well as kinesin into its pathway for ATP hydrolysis.

Kinetic and thermodynamic approaches allow investigation of specific questions about energy transduction for the actin motors, the microtubule motors, the RNA and DNA polymerases, and the DNA helicases. Information obtained from these studies allows us to determine which specific mechanistic features are general characteristics of molecular motors and which features must correlate with the specific behavior of a motor and its function in vivo. The results presented here provide new information about the interactions of dimeric Ncd with the microtubule. These studies have provided direct evidence that ADP product release is the slowest step in the pathway and that Ncd is not processive for ATP hydrolysis. Future experiments will examine cooperative interactions at the individual steps in the pathway to determine mechanistic contributions to directional bias and spindle dynamics in vivo.

ACKNOWLEDGMENT

We would like to thank Lori A. Bibb for performing the mantATP experiments with the pure isomers. We would also like to thank Andrew T. Mackey for helpful discussions and critical reading of the manuscript. Additionally, we are grateful to Sharyn Endow for providing the MC1 clone.

REFERENCES

1. Chandra, R., Salmon, E. D., Erickson, H. P., Lockhart, A., and Endow, S. A. (1993) *J. Biol. Chem. 268*, 9005−9013.
2. Endow, S. A., Henikoff, A., and Soler-Niedziela, L. (1990) *Nature 345*, 81−83.
3. McDonald, H. B., and Goldstein, L. S. B. (1990) *Cell 61*, 991−1000.
4. Vale, R. D., and Fletterick, R. J. (1997) *Annu. Rev. Cell Dev. Biol. 13*, 745−777.
5. Hirokawa, N. (1998) *Science 279*, 519−526.
6. Walker, R. A., Salmon, E. D., and Endow, S. A. (1990) *Nature 347*, 780−782.
7. McDonald, H. B., Stewart, R. J., and Goldstein, L. S. B. (1990) *Cell 63*, 1159−1165.
8. Stewart, R. J., Semerjian, J., and Schmidt, C. F. (1998) *Eur. Biophys. J. 27*, 353−360.
9. Case, R. B., Pierce, D. W., Hom-Booher, N. H., Hart, C. L., and Vale, R. D. (1997) *Cell 90*, 959−966.
10. DeCastro, M. J., Ho, C. H., and Stewart, R. J. (1999) *Biochemistry 38*, 5076−5081.
11. Howard, J., Hudspeth, A. J., and Vale, R. D. (1989) *Nature 342*, 154−158.
12. Gilbert, S. P., Webb, M. R., Brune, M., and Johnson, K. A. (1995) *Nature 373*, 671−676.
13. Kull, F. J., Sablin, E. P., Lau, R., Fletterick, R. J., and Vale, R. D. (1996) *Nature 380*, 550−555.
14. Sablin, E. P., Kull, F. J., Cooke, R., Vale, R. D., and Fletterick, R. J. (1996) *Nature 380*, 555−559.
15. Kozielski, F., Sack, S., Marx, A., Thormählen, M., Schönbrunn, E., Biou, V., Thompson, A., Mandelkow, E. M., and Mandelkow, E. (1997) *Cell 91*, 985−994.
16. Sablin, E. P., Case, R. B., Dai, S. C., Hart, C. L., Ruby, A., Vale, R. D., and Fletterick, R. J. (1998) *Nature 395*, 813−816.
17. Gilbert, S. P., Moyer, M. L., and Johnson, K. A. (1998) *Biochemistry 37*, 792−799.
18. Ma, Y.-Z., and Taylor, E. W. (1995) *Biochemistry 34*, 13242−13251.
19. Ma, Y. Z., and Taylor, E. W. (1997) *J. Biol. Chem. 272*, 724−730.
20. Pechatnikova, E., and Taylor, E. W. (1997) *J. Biol. Chem. 272*, 30735−30740.
21. Pechatnikova, E., and Taylor, E. W. (1999) *Biophys. J. 77*, 1003−1016.
22. Foster, K. A., Correia, J. J., and Gilbert, S. P. (1998) *J. Biol. Chem. 273*, 35307−35318.
23. Gilbert, S. P., and Johnson, K. A. (1993) *Biochemistry 32*, 4677−4684.
24. Hiratsuka, T. (1983) *Biochim. Biophys. Acta 742*, 496−508.
25. Woodward, S. K. A., Eccleston, J. F., and Geeves, M. A. (1991) *Biochemistry 30*, 422−430.
26. Shimizu, T., Sablin, E., Vale, R. D., Fletterick, R., Pechatnikova, E., and Taylor, E. W. (1995) *Biochemistry 34*, 13259−13266.
27. Gilbert, S. P., and Johnson, K. A. (1994) *Biochemistry 33*, 1951−1960.
28. Moyer, M. L., Gilbert, S. P., and Johnson, K. A. (1998) *Biochemistry 37*, 800−813.
29. Moore, J. D., Song, H., and Endow, S. A. (1996) *EMBO J. 15*, 3306−3314.
30. Lockhart, A., Cross, R. A., and McKillop, D. F. A. (1995) *FEBS Lett. 368*, 531−535.
31. Block, S. M., Goldstein, L. S. B., and Schnapp, B. J. (1990) *Nature 348*, 348−352.
32. Uyeda, T. Q. P., Warrick, H. M., Kron, S. J., and Spudich, J. A. (1991) *Nature 352*, 307−311.
33. Molloy, J. E., Burns, J. E., Kendrick-Jones, J., Tregear, R. T., and White, D. C. (1995) *Nature 378*, 209−212.
34. Finer, J. T., Simmons, R. M., and Spudich, J. A. (1994) *Nature 368*, 113−119.
35. Lymn, R. W., and Taylor, E. W. (1971) *Biochemistry 10*, 4617−4624.
36. Holzbaur, E. L. F., and Johnson, K. A. (1989) *Biochemistry 28*, 7010−7016.
37. Rosenfeld, S. S., and Taylor, E. W. (1984) *J. Biol. Chem. 259*, 11908−11919.
38. Hibberd, M. G., Dantzig, J. A., Trentham, D. R., and Goldman, Y. E. (1985) *Science 228*, 1317−1319.
39. Dantzig, J. A., Hibberd, M. G., Trentham, D. R., and Goldman, Y. E. (1991) *J. Physiol. (London) 432*, 639−680.
40. White, H. D., Belknap, B., and Webb, M. R. (1997) *Biochemistry 36*, 11828−11836.
41. Porter, M. E., and Johnson, K. A. (1983) *J. Biol. Chem 258*, 6582−6587.

BI991500B